

van der Waals Function for Molecular Mechanics

Li Yang, Lei Sun, and Wei-Qiao Deng*

Cite This: *J. Phys. Chem. A* 2020, 124, 2102–2107

Read Online

ACCESS |



Metrics & More

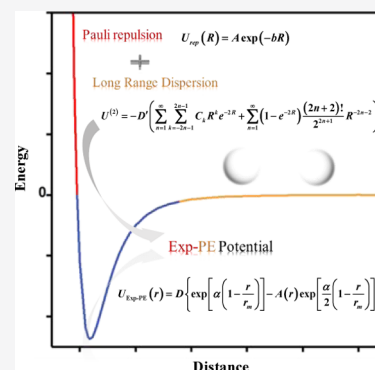


Article Recommendations



Supporting Information

ABSTRACT: van der Waals (vdW) interaction has been described with a Lennard-Jones potential for decades in molecular mechanics. Here, we report a new potential function Exp-PE from quantum mechanical derivation for vdW interactions for molecular mechanic simulation. High-order ab initio calculations and experimental atomic force microscopy measurements have been used to test its feasibility, and the results suggest that this formula is simple, accurate, and transferable. This new potential function is capable of upgrading the traditional force fields especially for the applications involving vdW interactions.



1. INTRODUCTION

van der Waals (vdW) interactions are of fundamental importance for understanding the dynamic and static properties of gases, liquids, and solids. In molecular mechanics, these interactions have usually been expressed as a classical potential function containing repulsion and dispersion components.^{1–6} Traditional force fields usually describe vdW interactions with the Lennard-Jones (LJ) 12-6 potential,^{3–6} considering that the long-range dispersion interaction can be approximated as $1/R^{-6}$. However, this form is not a sacred law of physics but just the result of approximations in many different ways by various authors,^{7–11} and the original authors admit that this form is only applicable for quite large distances. Moreover, a cutoff of approximately 10 Å is usually needed for the vdW interactions in the force field to reduce the computational cost. Under this restriction, $1/R^{-6}$ may not be the only reasonable form. In addition, the inverse power term ($1/R^n$) of the LJ potential is known to make the inner wall too stiff, thus causing problems in many computer simulations. The most direct problem is that the short distance energy between atoms or molecules cannot be reproduced. The potential diverges when two atoms approach one another, which may create instability. As early as 1963, Gambhir and Saxena^{12,13} proposed that the LJ potential is somewhat incorrect in correlating the equilibrium properties of gases and gaseous mixtures. Hart and Rappé¹⁴ in 1992 also declared the limits of the LJ and Exp-6 (Buckingham) potentials in describing the full range of vdW interactions, and they suggested using the Morse potential at the same time. Goddard et al.^{15–17} further used the Morse potential in predicting gas adsorption in porous frameworks and obtained reliable simulation results. However, our experience usually shows that although the Morse potential is more suitable for describing the interaction of repulsive regions, its long-range

exponential form always decays much faster than the actual vdW interaction does with increasing distance.

Here, we propose a new function for vdW interactions that can accurately describe both the repulsion and dispersion components of vdW interactions for application in molecular mechanics. Ab initio methods and atomic force microscopy (AFM) measurements have been used to test the performance of the potential function. The overall performance is benchmarked against ab initio quantum mechanical (QM) calculations. We illustrate that the new function produces accurate vdW interactions, both for QM calculations and AFM measurements.

2. METHODS

The Thomas–Fermi–Dirac statistical and self-consistent-field theories give reliable results that the vdW repulsion energy (V_{rep}) can be very well fitted by a simple exponential Born–Mayer term,^{18,19} $V_{\text{rep}}(R) = A \exp(-bR)$, where A and b are constants. Starting from the Schrodinger equation and taking H_2 as a model system, we deduce the expression of the ground state energy of H_2 at a larger distance. We solve the ground state energy of H_2 with the Hamiltonian

Received: December 3, 2019

Revised: December 23, 2019

Published: January 21, 2020

$$\hat{H} = -\frac{1}{2}(\nabla_1^2 + \nabla_2^2) + \frac{1}{r_{12}} - \left(\frac{1}{r_{a1}} + \frac{1}{r_{a2}} + \frac{1}{r_{b1}} + \frac{1}{r_{b2}} \right) + \frac{1}{R} \quad (1)$$

where “1” and “2” refer to electrons one and two, “a” and “b” refer to two H nuclei, R and r_{12} are the distances between the two H nuclei and two electrons, respectively, and r_{a1} , r_{a2} , r_{b1} , and r_{b2} are the distances between the H nuclei and electrons. The system is supposed to be in the ground state. The atomic hydrogen orbitals are given by

$$\psi(r) = \frac{\lambda^{3/2}}{\sqrt{\pi}} \exp[-\lambda r] \quad (2)$$

where λ is the effective charge. The ground state wave function for H_2 can be treated as

$$\Psi_{H_2} = [\psi(r_{a1})\psi(r_{b2}) + \psi(r_{a2})\psi(r_{b1})] \quad (3)$$

The corresponding energies in terms of the ground state wave function are

$$E_{H_2} = \frac{1}{R} + \frac{2(A + A's)}{1 + s^2} - \frac{2(\kappa + \varepsilon s) - (\kappa' + \varepsilon')}{1 + s^2} \quad (4)$$

where s is the overlap integral, κ and κ' are the coulomb integrals, and A corresponds to the ground state energy of one H atom. A and κ' are independent of s and can be understood by classical images. The energies ε , ε' , and A' are caused by exact quantum effects (exchange effects) and have no corresponding classical images. Using $\rho = \lambda R$, specific expressions for s , A , κ , κ' , ε , ε' , and A' can be found, as shown in the Supporting Information (eqs S10–S14, S16, and S17). Assuming that the exponential integral $E_1(\rho)$ (eq S19) and the overlap integral s^2 are small enough to be negligible, E_s can be expressed as follows

$$E_{H_2} = 2A + (C_{-1}\rho^{-1} + C_0\rho^0 + C_1\rho^1 + C_2\rho^2 + C_3\rho^3 + C_4\rho^4)\exp(-2\rho) \quad (5)$$

Equation 5 illustrates that the ground state energy of H_2 can be approximated in the form of a series multiplied by exponents when R is large enough. The similar results can also be found in other works.^{14,20}

A similar function can also be derived from the H_2^+ system (see the Supporting Information)

$$E_{H_2^+} = -\frac{1}{\varepsilon} \left(\sum_{n=1}^{\infty} \sum_{k=-2n-1}^{2n-1} C_k R^k e^{-2R} + \sum_{n=1}^{\infty} (1 - e^{-2R}) \frac{(2n+2)!}{2^{2n+1}} R^{-2n-2} \right) + \text{Con.} \quad (6)$$

When R is large enough, $(1 - e^{-2R}) \cong 1$, and the first term of eq 6 can be approximated as 0. As R decreases, the exponential term is increasingly important; ignoring the other terms makes R^{-2n-2} dominant, leading to the potential diverging to negative infinity. According to eq 6, when R is large enough, the dispersion can be approximately with asymptotic multipole expansion, but when simply add the expansion with the Born–Mayer term,^{18,19} it will cause the potential to dive toward negative infinity like Exp-6 potential.¹⁴ One way to deal with this problem is introducing in damping function as Tang and Toennies et al. did.^{21–24} However, the

form of the damping function such as Tang and Toennies is too complicate to be used in a molecular mechanic force field. Actually, the divergence of the short-range can be avoided by keeping the exponential term as the determinate term in the cut-off range of the force field without considering the series expansion form of the long-range dispersion. However, the decay rate of exponential is much faster than multipole expansion. In order to compensate for the too faster decay rate of the exponential term, we introduced a series correction to the term of attraction. Assume that the vdW potential function has the form of eq 7.

$$U(r) = \varepsilon \{ \exp[\alpha(1 - r/r_m)] - A(r) \exp[\alpha/2(1 - r/r_m)] \} \quad (7)$$

where ε is the well depth, r_m is the interatomic distance at the energy minimum, and $A(r)$ is a polynomial that slows down the decay of the exponential.

Note that the new function must meet two basic conditions, $U(r = r_m)/\varepsilon = -1$ and $dU/dr|_{r=r_m} = 0$. In addition, two additional constraints exist, $\lim_{r \rightarrow \infty} A(r) = \infty$ and $\lim_{r \rightarrow 0} A(r) = \text{constant}$. To make the potential functional form as simple as possible, no parameters other than ε , α , and r_m should be contained in $A(r)$. Combining the four constraints and eq 5, we propose a very simple form for $A(r)$

$$A(r) = (r/r_m)^{2n} - 2(r/r_m)^n + 3 \quad (8)$$

where n is an integer. Equation 7 recovers the Morse potential when $n = 0$, and our results suggest that it performs best when $n = 2$.

Thus, we obtain the final form, named Exp-PE

$$U_{\text{Exp-PE}}(r) = \varepsilon \{ \exp[\alpha(1 - r/r_m)] - ((r/r_m)^4 - 2(r/r_m)^2 + 3) \times \exp[\alpha/2(1 - r/r_m)] \} \quad (9)$$

The thought of this formula is somewhat similar to the damping function series such as Tang and Toennies in introducing the revision form. Tang's function^{21–24} is to modify the short-range divergence of series expansion by introducing the damping function, while the that of Exp-PE is to modify the exponential long-range dispersion by introducing the series. The Exp-PE potential function is very simple and only has three parameters need to be fitted like Morse potential does. Additionally, it fixed a bug of the vdW potential function in the molecular mechanical force field and could be used to improve the accuracy of the most molecular simulations.

3. RESULTS AND DISCUSSION

Many systems are bound together by vdW interactions; but among them, noble gas dimers prominently stand out. The CCSD(T) approach^{25,26} extrapolated to the complete basis set (CBS) limit, that is, CCSD(T)/CBS, has been carried out for He–Ar and Ar–Ar dimers to provide a numerical test of the Morse, Exp-PE and LJ 12-6 potentials. The augmented, correlation consistent basis sets aug-cc-pV5Z and aug-cc-pV6Z were utilized.^{27,28} Basis set superposition errors (BSSEs) were accounted for using the counterpoise method.^{29,30} An extrapolation to the CBS limit for the electronic correlation energy was performed using a two-point extrapolation scheme according to Helgaker et al.³¹ The related extrapolated formula is written as

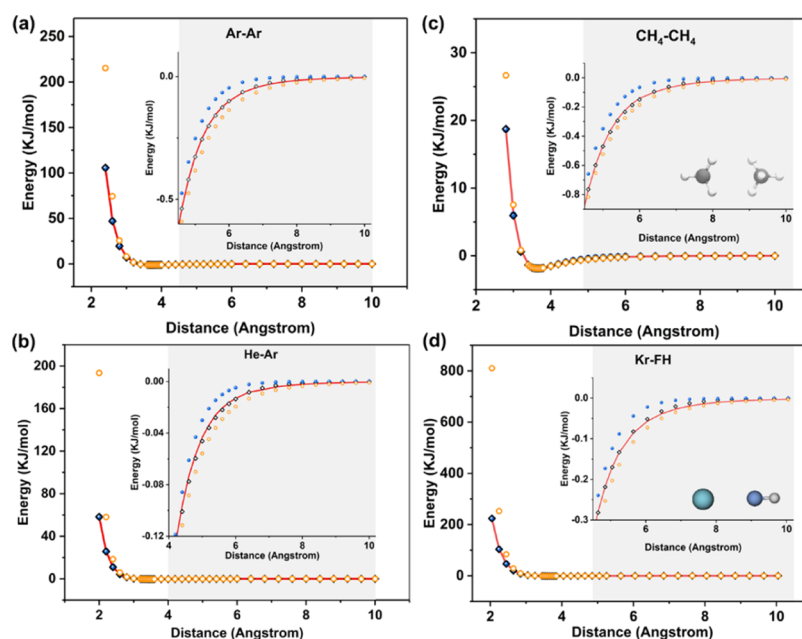


Figure 1. Comparison of the fitted energies with QM results: (a) Ar–Ar, (b) He–Ar, (c) CH₄–CH₄, and (d) Kr–FH. Here, C atoms are brown, H white, F ice blue, and Kr dark cyan. QM results are shown as a solid red line while fitting energies with different potential function are shown in symbols. Blue balls: Morse; black rhombus: Exp-PE; and orange circles: LJ 12-6. Distance for (c) is the separation between geometrical centers, while for (d) it is the separation between the centers of mass.

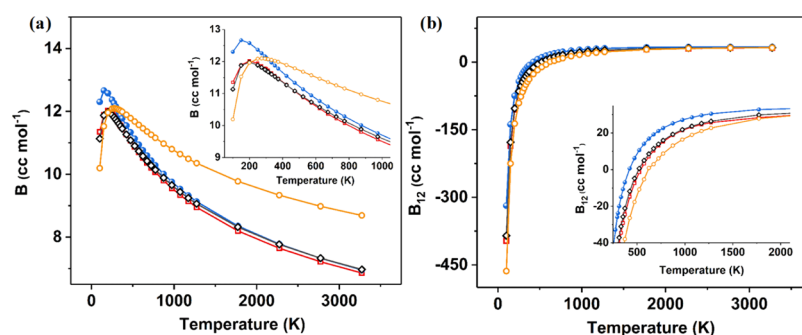


Figure 2. Comparisons of experimental and calculated second virial coefficients. Second virial coefficients are shown as a function of temperature for the (a) He–He and (b) Xe–Ar systems. Red square: QM results; Blue balls: Morse; black rhombus: Exp-PE; and orange circles: LJ 12-6.

$$E_{\text{corr}}^X = E_{\text{corr}}^{\text{CBS}} + C/X^3 \quad (10)$$

where X is the cardinal number of the basis sets (aug-cc-PV5Z: 5, aug-cc-PV6Z: 6), E_{corr}^X is the correlation energy obtained with the basis set with cardinal number X , $E_{\text{corr}}^{\text{CBS}}$ is the basis set limit of the correlation energy, and C is a constant. The HF energy converges much faster than the correlation energy with respect to the size of the atomic basis set. Thus, to simplify, the HF limit is directly taken from the aug-cc-pV6Z basis set.

Figure 1a,b shows comparisons of the new function with the LJ 12-6 and Morse potentials in terms of reproducing the QM potential curve of Ar–Ar and He–Ar noble gas pairs. Fitting parameters are listed in Table S2. We obtained excellent agreement with QM calculations, and the agreement is very good considering that the new function is very simple. In sharp contrast to the other two functions, Exp-PE nearly matches the reference potentials for all values of R . The Morse potential performs well for the short-range repulsion but significantly deviates from the QM energy for the middle and long-range dispersion. LJ 12-6 reproduces the behavior of long-range attractive interactions much better than the Morse potential,

but it shows a significant deviation for the repulsive interactions.

In addition to rare gases, we further explored other intermolecular interactions. Figure 1c,d shows the potentials for the nonpolar system (CH₄–CH₄) and the polar system HF–Kr. The CCSD(T)/QZVPP level was used here. We discussed the relationship between fitting accuracy and QM calculation levels in Supporting Information. As shown in Figures S1 and S3, different calculation levels have significant influence on the energy of the potential well, while the influence on the fitting accuracy can be nearly ignored.

The same as in the case of noble gas dimers, the Morse potential failed describing the potential in the region of the asymptotic part and LJ 12-6 potential failed reproducing the repulsion of the potential curves. As shown in the insets of Figure 1, the Exp-PE potential even reproduces the attraction part of the potential curves better than LJ 12-6 potential. This is an important result. For a long time, LJ 12-6 has been widely used. In addition to its simple enough form, it has advantages in describing attraction of vdW interactions. However, the advantages of LJ 12-6 in describing attraction are not superior

to Exp-PE potential. In summary, for all of the investigated systems, the new form of the dispersion in Exp-PE that clearly made the overall performance significantly improved.

The second virial coefficient ($B(T)$) is often used for testing the reliability and appropriateness of potential functions because of its enhanced sensitivity to the law of molecular interactions. The calculated and experimental³² second virial coefficients of two noble gas dimers, He–He and Xe–Ar, are shown in Figure 2. In order to ensure the calculation accuracy of the second virial coefficient, we considered scalar relativistic effects via a second-order Douglas–Kroll–Hess approximation for the energy calculation of the Xe–Ar system.³³ Douglas–Kroll correlation consistent polarized valence basis set, aug-cc-pVTZ-DK and aug-cc-pVQZ-DK were utilized for Xe–Ar energy extrapolation.^{34,35} We have extended the calculations of $B(T)$ to a very high temperature (3273.15 K), where the dispersion will be dominant. The parameters used to calculate second virial coefficients are listed in Table S2. For the He–He systems, the values calculated with the LJ 12-6 potential diverge considerably from the experimental values, where the discrepancies are systematic and slightly more than those that can be explained on the basis of uncertainties in the experiments. This result may be attributed to defects of the function itself. Figure 2a,b clearly shows that our new function (Exp-PE) has a significant correction in describing $B(T)$ compared with the Morse and LJ 12-6 potentials whether at high or low temperatures. This result is consistent with the accuracy in describing vdW interactions, as shown in Figure 1.

To benchmark the performance of the functional forms (see Table S3) for vdW interactions, we calculated 419 data points in the attractive region and 90 data points in the repulsive region for 15 vdW systems. The 15 prototypic systems included 9 rare gas diatomic molecules (Ne–Ne, Ar–Ar, Kr–Kr, He–Ne, He–Ar, He–Kr, Ne–Ar, Ne–Kr, and Ar–Kr), 4 small-molecule gas pairs (H_2-H_2 , N_2-N_2 , CH_4-CH_4 , and O_2-O_2) and 2 polarity systems (LiH–He and HF–Kr). The configuration interactions of the nine rare gas diatomic molecules were calculated at the CCSD(T)/aug-cc-pv5z level, while the other systems were calculated at the CCSD(T)/QZVPP level. All binding energies in the binary systems were corrected using the BSSEs by the full counterpoise procedure.^{29,30} The well depth ϵ and minimum-energy position r_m were directly extrapolated from the ab initio calculations during the fitting process. The parameters are listed in Table 1. The mean absolute deviations (MADs) for the different functional forms are graphically displayed in Figure 3. The enhancement of Exp-PE over the other functional forms is evident. The MAD for attraction decreases in the range from 16% (compared to Exp-6) to 44% (compared to the Morse potential). This result corresponds to an important correction for the attractive interactions. As shown in Figure 3, the difference in the MADs between potential functions in the repulsive region is even more significant. The MAD for the LJ 12-6 potential in the repulsive region is too large to be overlooked. This result further confirms that the LJ potential is too rigid to describe the full range of vdW interactions. Morse and Morse-4-2 perform consistently in the repulsive region because both potentials can reduce to the Born–Mayer term at a short distance.

The interaction between the tip and the sample can be directly measured with AFM to the atomic scale based on the frequency shift of an oscillating cantilever.³⁶ Kawai et al. measured the vdW interactions at the atomic-scale contacts of

Table 1. Parameters of Potential Functions Developed To Fit the CCSD(T) Calculations

systems	LJ 12-6/Buf-14-7		α		
	ϵ (KJ mol ⁻¹)	r_m (Å)	Exp-6	Morse	Exp-PE
Ne–Ne ^a	0.31	3.13	14.47	13.66	13.70
Ar–Ar ^a	1.09	3.80	13.23	12.64	12.67
Kr–Kr ^a	1.52	4.10	13.14	12.54	12.59
He–Ne ^a	0.16	3.05	13.77	13.11	13.15
He–Ar ^a	0.23	3.50	13.92	13.19	13.24
He–Kr ^a	0.23	3.70	14.08	13.29	13.35
Ne–Ar ^a	0.50	3.50	14.36	13.48	13.54
Ne–Kr ^a	0.53	3.70	14.16	13.28	13.36
Ar–Kr ^a	1.27	3.80	13.60	12.91	12.97
H ₂ –H ₂ ^b	0.31	3.43	12.10	11.49	11.68
N ₂ –N ₂ ^b	0.95	4.25	14.73	13.61	13.72
CH ₄ –CH ₄ ^b	1.87	3.65	13.63	11.19	12.79
O ₂ –O ₂ ^b	1.48	3.35	11.76	11.19	11.41
HF–Kr ^b	0.71	3.70	13.90	11.24	13.19
LiH–He ^b	1.67	2.30	11.75	11.24	11.38

^aCCSD(T)/aug-cc-pv5z. ^bCCSD(T)/qzvpp.

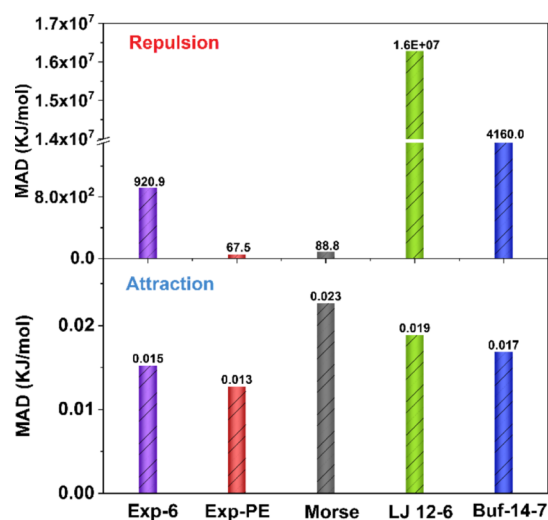


Figure 3. Comparison of MAD values for different functional forms in repulsion (Repul.) and attraction (Attr.) regions.

Xe–Ar, Xe–Kr, and Xe–Xe atoms.³⁷ To provide a comparative test of the Exp-PE potential function, their experimental data are used for fitting. As shown in Figure 4, only the data in the range of $r > r_m$ are employed. The measured vdW interactions contain two parts. One is the interaction between the tip and the rare gas atom on the surface, and the other is the interaction between the Xe atom adsorbed on the tip and the rare gas atom on the surface. Only the second one is the ideal interaction we want to consider. The authors confirmed that the contribution of the tip-noble atom interaction can be neglected compared with the interaction between Xe and the noble atom. However, when the z distance is not large enough, this approximation will cause significant deviations because the two parts of the vdW interactions have very different mathematic laws. As shown in Figure 4, the new potential function Exp-PE can nearly perfectly reproduce the experimental potential curves of Xe–Ar, Xe–Kr, and Xe–Xe. Fitting parameters are listed in Table S4. The vdW interaction measured by Kawai et al. is not the interaction between the two isolated neutral rare gas atoms.

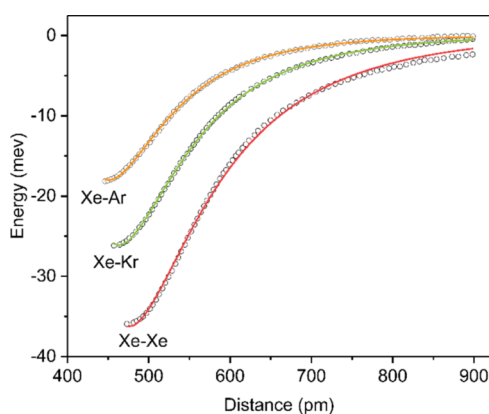


Figure 4. Fit of the Exp-PE potential to experimental potential curves. Experimental curves are marked with open circles, and fitted curves are marked with full lines.

The atoms adsorbed at the tip and the surface have a certain polarization, and the measured vdW interactions include polarization interactions. This phenomenon is why the interactions they measured are several times larger than the pure atom–dimer interaction curves. Testing the vdW potential energy function with such data is meaningful. Atoms in the vdW interaction systems we usually deal with, such as a stack of base pairs, will be more or less affected by the surrounding environment and produce a certain degree of polarization. If a functional form can describe the vdW interactions between atoms in various environments, it will have a wider use.

4. CONCLUSIONS

In conclusion, we recalculated the form of the long-range dispersion by using H_2 systems to give a more fundamental understanding. The results suggest that a power series expansion is suitable for a large distance, where the exponential part can be neglected. However, ignoring the exponential form in the middle or short range will cause a significant deviation, as the electron overlap function is non-negligible in this case. Based on the mathematical and physical constraints, we proposed a simple potential function, Exp-PE, for vdW interactions. Test results show that Exp-PE has a significant correction compared to other commonly used force field functional forms in describing vdW interactions. The test results show that Exp-PE has a significant correction compared to the LJ 12-6 and Morse functional forms in describing vdW interactions. Exp-PE can reproduce the asymptotic behavior up to 10 Å, which is sufficient for most molecular mechanics simulations. Moreover, AFM measurements further indicate that the new function deals with the systems that contain polarization very well. Therefore, we have provided a possible accurate description of both the repulsion and dispersion in vdW interactions using a simple potential function that will hopefully be wider utilized in applications. This work may also provide a new idea for finding more suitable and simpler vdW functional forms.

■ ASSOCIATED CONTENT

Supporting Information

The Supporting Information is available free of charge at <https://pubs.acs.org/doi/10.1021/acs.jpca.9b11222>.

Effect of the accuracy of ab initio calculation for fitting results; terms and parameters for different vdW potential functions; integral method of second virial coefficient; and details of derivation process (PDF)

■ AUTHOR INFORMATION

Corresponding Author

Wei-Qiao Deng — State Key Laboratory of Molecular Reaction Dynamics, Dalian National Laboratory for Clean Energy, Dalian Institute of Chemical Physics, Chinese Academy of Sciences, Dalian 116023, China; Institute of Molecular Sciences and Engineering, Institute of Frontier and Interdisciplinary Science, Shandong University, Qingdao 266237, China; orcid.org/0000-0002-3671-5951; Email: dengwq@sdu.edu.cn

Authors

Li Yang — State Key Laboratory of Molecular Reaction Dynamics, Dalian National Laboratory for Clean Energy, Dalian Institute of Chemical Physics, Chinese Academy of Sciences, Dalian 116023, China; Institute of Molecular Sciences and Engineering, Institute of Frontier and Interdisciplinary Science, Shandong University, Qingdao 266237, China; University of the Chinese Academy of Sciences, Beijing 100039, China

Lei Sun — Institute of Molecular Sciences and Engineering, Institute of Frontier and Interdisciplinary Science, Shandong University, Qingdao 266237, China

Complete contact information is available at:

<https://pubs.acs.org/doi/10.1021/acs.jpca.9b11222>

Notes

The authors declare no competing financial interest.

■ ACKNOWLEDGMENTS

This work was supported by the National Key Research and Development Program of China (no. 2017YFA0204800), the National Science and Technology Major Project of the Ministry of Science and Technology of China (no. 2017ZX05036001), the National Natural Science Foundation of China (nos. 21525315 and 21721004), Chinese Academy of Sciences (no. XDB10020201), and the Fundamental Research Funds of Shandong University, the National Key Research (no. 2019HW016).

■ REFERENCES

- (1) Van Duin, A. C. T.; Dasgupta, S.; Lorant, F.; Goddard, W. A., III ReaxFF: a reactive force field for hydrocarbons. *J. Phys. Chem. A* **2001**, *105*, 9396–9409.
- (2) Molinero, V.; Goddard, W. A., III M3B: A coarse grain force field for molecular simulations of malto-oligosaccharides and their water mixtures. *J. Phys. Chem. B* **2004**, *108*, 1414–1427.
- (3) Mayo, S. L.; Olafson, B. D.; Goddard, W. A., III DREIDING: A Generic Force Field for Molecular Simulations. *J. Phys. Chem.* **1990**, *94*, 8897–8909.
- (4) Rappe, A. K.; Casewit, C. J.; Colwell, K. S.; Goddard, W. A., III; Skiff, W. M. UFF, a full periodic table force field for molecular mechanics and molecular dynamics simulations. *J. Am. Chem. Soc.* **1992**, *114*, 10024–10035.
- (5) Sun, H.; Mumby, S. J.; Maple, J. R.; Hagler, A. T. An ab initio CFF93 all-atom force field for polycarbonates. *J. Am. Chem. Soc.* **1994**, *116*, 2978–2987.
- (6) Hagler, A.; Huler, E.; Lifson, S. Energy functions for peptides and proteins. I. Derivation of a consistent force field including the

hydrogen bond from amide crystals. *J. Am. Chem. Soc.* **1974**, *96*, 5319–5327.

(7) Slater, J. C.; Kirkwood, J. G. The van der Waals forces in gases. *Phys. Rev.* **1931**, *37*, 682.

(8) Margenau, H. Quadrupole Contributions to London's Dispersion Forces. *J. Chem. Phys.* **1938**, *6*, 896–899.

(9) Brooks, F. C. Convergence of intermolecular force series. *Phys. Rev.* **1952**, *86*, 92.

(10) Roe, G. M. Convergence of intermolecular force series. *Phys. Rev.* **1952**, *88*, 659.

(11) Dalgarno, A.; Lewis, J. T. The representation of long range forces by series expansions I: The divergence of the series II: The complete perturbation calculation of long range forces. *Proc. Phys. Soc., London, Sect. A* **1956**, *69*, 57.

(12) Gambhir, R. S.; Saxena, S. C. Zero Pressure Joule-Thomson Coefficient for a Few Non-Polar Gases on the Morse Potential. *Indian J. Phys.* **1963**, *37*, 540–542.

(13) Saxena, S. C.; Gambhir, R. S. Second virial coefficient of gases and gaseous mixtures on the Morse potential. *Mol. Phys.* **1963**, *6*, 577–583.

(14) Hart, J. R.; Rappé, A. K. van der Waals functional forms for molecular simulations. *J. Chem. Phys.* **1992**, *97*, 1109–1115.

(15) Mendoza-Cortés, J. L.; Han, S. S.; Furukawa, H.; Yaghi, O. M.; Goddard, W. A., III Adsorption mechanism and uptake of methane in covalent organic frameworks: theory and experiment. *J. Phys. Chem. A* **2010**, *114*, 10824–10833.

(16) Sun, L.; Yang, L.; Zhang, Y.-D.; Shi, Q.; Lu, R.-F.; Deng, W.-Q. Accurate van der Waals force field for gas adsorption in porous materials. *J. Comput. Chem.* **2017**, *38*, 1991–1999.

(17) Han, S. S.; Kim, D.; Jung, D. H.; Cho, S.; Choi, S.-H.; Jung, Y. Accurate ab initio-based force field for predictive CO₂ uptake simulations in MOFs and ZIFs: Development and applications for MTV-MOFs. *J. Phys. Chem. C* **2012**, *116*, 20254–20261.

(18) Dick, B. G.; Overhauser, A. W. Theory of the dielectric constants of alkali halide crystals. *Phys. Rev.* **1958**, *112*, 90.

(19) Hafemeister, D. W.; Zahrt, J. D. Exchange-Charge-Model Calculation of the Born-Mayer Repulsive Potential in Ionic Gases and Crystals. *J. Chem. Phys.* **1967**, *47*, 1428–1437.

(20) Koide, A. A new expansion for dispersion forces and its application. *J. Phys. B: At. Mol. Phys.* **1976**, *9*, 3173–3183.

(21) Tang, K. T.; Toennies, J. P. A simple theoretical model for the van der Waals potential at intermediate distances. I. Spherically symmetric potentials. *J. Chem. Phys.* **1977**, *66*, 1496–1506.

(22) Tang, K. T.; Toennies, J. P. A simple theoretical model for the van der Waals potential at intermediate distances. II. Anisotropic potentials of He-H₂ and Ne-H₂. *J. Chem. Phys.* **1978**, *68*, 5501–5517.

(23) Tang, K. T.; Toennies, J. P. A simple theoretical model for the van der Waals potential at intermediate distances. III. Anisotropic potentials of Ar-H₂, Kr-H₂, and Xe-H₂. *J. Chem. Phys.* **1981**, *74*, 1148–1161.

(24) Bowers, M. S.; Tang, K. T.; Toennies, J. P. The anisotropic potentials of He-N₂, Ne-N₂, and Ar-N₂. *J. Chem. Phys.* **1988**, *88*, 5465–5474.

(25) Purvis, G. D.; Bartlett, R. J. A full coupled-cluster singles and doubles model: The inclusion of disconnected triples. *J. Chem. Phys.* **1982**, *76*, 1910–1918.

(26) Pople, J. A.; Head-Gordon, M.; Raghavachari, K. Quadratic configuration interaction. A general technique for determining electron correlation energies. *J. Chem. Phys.* **1987**, *87*, 5968–5975.

(27) Woon, D. E.; Dunning, T. H., Jr. Gaussian basis sets for use in correlated molecular calculations. IV. Calculation of static electrical response properties. *J. Chem. Phys.* **1994**, *100*, 2975–2988.

(28) Van Mourik, T.; Wilson, A. K.; Dunning, T. H., Jr. Benchmark calculations with correlated molecular wavefunctions. XIII. Potential energy curves for He₂, Ne₂ and Ar₂ using correlation consistent basis sets through augmented sextuple zeta. *Mol. Phys.* **1999**, *96*, 529–547.

(29) Simon, S.; Duran, M.; Dannenberg, J. J. How does basis set superposition error change the potential surfaces for hydrogen-bonded dimers? *J. Chem. Phys.* **1996**, *105*, 11024–11031.

(30) Boys, S. F.; Bernardi, F. The calculation of small molecular interactions by the differences of separate total energies. Some procedures with reduced errors. *Mol. Phys.* **1970**, *19*, 553–566.

(31) Halkier, A.; Helgaker, T.; Jørgensen, P.; Klopper, W.; Koch, H.; Olsen, J.; Wilson, A. K. Basis-set convergence in correlated calculations on Ne, N₂, and H₂O. *Chem. Phys. Lett.* **1998**, *286*, 243–252.

(32) Kestin, J.; Knierim, K.; Mason, E. A.; Najafi, B.; Ro, S. T.; Waldman, M. Equilibrium and transport properties of the noble gases and their mixtures at low density. *J. Phys. Chem. Ref. Data* **1984**, *13*, 229–303.

(33) De Jong, W. A.; Harrison, R. J.; Dixon, D. A. Parallel Douglas–Kroll energy and gradients in NWChem: Estimating scalar relativistic effects using Douglas–Kroll contracted basis sets. *J. Chem. Phys.* **2001**, *114*, 48.

(34) Bross, D. H.; Peterson, K. A. Correlation consistent, Douglas–Kroll–Hess relativistic basis sets for the 5p and 6p elements. *Theor. Chem. Acc.* **2014**, *133*, 1434.

(35) Woon, D. E.; Dunning, T. H. Gaussian basis sets for use in correlated molecular calculations. III. The atoms aluminum through argon. *J. Chem. Phys.* **1993**, *98*, 1358–1371.

(36) Lantz, M. A.; Hug, H. J.; Hoffmann, R.; Van Schendel, P. J. A.; Kappenberger, P.; Martin, S.; Baratoff, A.; Güntherodt, H. J. Quantitative measurement of short-range chemical bonding forces. *Science* **2001**, *291*, 2580–2583.

(37) Kawai, S.; Foster, A. S.; Björkman, T.; Nowakowska, S.; Björk, J.; Canova, F. F.; Gade, L. H.; Jung, T. A.; Meyer, E. Van der Waals interactions and the limits of isolated atom models at interfaces. *Nat. Commun.* **2016**, *7*, 11559.